


Inactivation of *TMEM106A* promotes lipopolysaccharide-induced inflammation via the MAPK and NF- κ B signaling pathways in macrophages

X. Zhang,^{*†‡} T. Feng,[§] X. Zhou,[§]
P. M. Sullivan,[§] F. Hu,[§] Y. Lou,[¶] J. Yu,^{*†}
J. Feng,^{*†} H. Liu^{*} and Y. Chen ^{*†††}

^{*}Department of Immunology, Peking University School of Basic Medical Sciences, China, [†]NHC Key Laboratory of Medical Immunology, Peking University, [‡]Beijing Key Laboratory for Pediatric Diseases of Otolaryngology, Head and Neck Surgery, MOE Key Laboratory of Major Diseases in Children, Beijing Pediatric Research Institute, Beijing Children's Hospital, Capital Medical University, National Center for Children's Health (NCCH), Beijing, [§]Weill Institute for Cell and Molecular Biology, Department of Molecular Biology and Genetics, Cornell University, Ithaca, NY USA, [¶]Medical and Healthy Analytical Center, Peking University, ^{**}Department of Geriatrics, Peking University Third Hospital, and ^{††}Center for Human Disease Genomics, Peking University, Beijing

Accepted for publication 17 September 2020

Correspondence: H. Liu, Department of geriatrics, Peking University Third Hospital, Beijing 100191, China.

E-mail: zhouwlin@163.com

or

Y. Chen, Department of Immunology, Peking University School of Basic Medical Sciences; NHC Key Laboratory of Medical Immunology, Peking University, Beijing, 100191, China.

E-mail: yingyu_chen@bjmu.edu.cn

Introduction

Monocytes/macrophages are present in almost all tissues and play important roles in the maintenance of tissue homeostasis. Furthermore, they are essential components of the innate immune system and have a central role in inflammation and host defense [1,2]. They can rapidly change their function

Summary

Pattern recognition receptors, such as Toll-like receptors (TLRs), play an important role in the host defense against invading microbial pathogens. Their activation must be precisely regulated, as inappropriate activation or overactivation of TLR signaling pathways may result in inflammatory disorders, such as septic shock or autoimmune diseases. TMEM106A is a type II transmembrane protein constitutively expressed in macrophages. Our current study demonstrated that TMEM106A levels were increased in macrophages upon lipopolysaccharide (LPS) stimulation, as well as in the peripheral monocytes of patients with sepsis. *Tmem106a* knockout mice were more sensitive to lipopolysaccharide (LPS)-induced septic shock than wild-type mice. Further experiments indicated that *Tmem106a* ablation enhanced the expression of CD80, CD86 and major histocompatibility complex (MHC)-II in mouse macrophages upon LPS stimulation, accompanied with up-regulation of tumor necrosis factor (TNF)- α , interleukin (IL)-6, interferon (IFN)- β and inducible nitric oxide synthase (iNOS), indicating the activation of macrophages and polarization towards the M1 inflammatory phenotype. Moreover, elevated mitogen-activated protein kinase (MAPK) and nuclear factor kappa B (NF- κ B) signaling were found to be involved in the LPS-induced inflammatory response in *Tmem106a*^{-/-} macrophages. However, this effect was largely abrogated by macrophage deletion in *Tmem106a*^{-/-} mice. Therefore, deficiency of *Tmem106a* in macrophages may enhance the M1 polarization in mice, resulting in inflammation. This suggests that TMEM106A plays an important regulatory role in maintaining macrophage homeostasis.

Keywords: inflammation, lipopolysaccharide, macrophage, TMEM106A

in response to local microenvironmental signals. However, if inflammatory macrophage activation is not tightly controlled, it can contribute to many chronic inflammatory and autoimmune diseases [3,4]. How macrophages, a type of heterogeneous immunocyte with plasticity and pluripotency, maintain body homeostasis requires further research.

Pattern recognition receptors, such as Toll-like receptors (TLRs), localized at the cell surface help macrophages to detect bacterial infection and initiate innate immune responses to clear invading pathogens [5]. TLR-4 interacts with myeloid differentiation-2 (MD2) and CD14 to recognize lipopolysaccharide (LPS) and activates the myeloid differentiation primary response 88 (MyD88)-dependent and -independent signaling pathways and other downstream pathways, such as mitogen-activated protein kinase (MAPK) and nuclear factor kappa B (NF- κ B) pathways to induce downstream factors, including proinflammatory factors [such as interleukin (IL)-1 α , IL-1 β , IL-6 and tumor necrosis factor- α (TNF)], thus, initiating innate immune responses [6–10]. However, excessive or abnormal activation of TLR-4 can cause various acute and chronic diseases, such as septic shock and autoimmune diseases [11–13]. Therefore, the activation and function of TLR-4 must be precisely regulated to prevent excessive inflammatory responses leading to immune damage. Studies have shown that several negative regulatory molecules regulate the TLR-4-induced inflammatory process. For example, signaling lymphocyte activation molecule family (SLAMF)8 and SLAMF9, members of the SLAM family of transmembrane receptors, have been shown to enhance the secretion of inflammatory cytokines by up-regulating the expression of TLR-4 [14]. Moreover, autocrine–paracrine prostaglandin E₂ and its receptor EP4 were shown to restrict TIR-domain-containing adapter-inducing IFN- β (TRIF)-dependent signals and production of interferon (IFN)- β through regulation of TLR-4 internalization and trafficking [15]. An E3 ubiquitin-protein ligase, Triad3A, interacts with TLR-4 and promotes substantial degradation of TLR-4 with a concomitant decrease in signaling [16]. In addition, certain intracellular proteins, such as Src homology 2 (SH2) domain-containing phosphatase 2 (SHP2) and SH-2 containing inositol 5' polyphosphatase 1 (SHIP1) (phosphatases), A20 (de-ubiquitinating enzyme) and suppressor of cytokine signaling 1 (SOCS1) (E3 ubiquitin ligase) have been shown to negatively regulate the TLR-4 signaling pathway [17–19]. These negative regulatory molecules play an important role in maintaining immune homeostasis.

Transmembrane protein 106A (TMEM106A) is a novel protein implicated in human tumor progression previously identified by our group [20]. TMEM106A expression has been shown to be decreased in gastric cancer, renal cancer and non-small-cell lung carcinoma [20–22], and restoration of its expression can significantly inhibit tumor cell proliferation and induce cell death. *TMEM106A* is evolutionarily conserved, and its homologs are present in mice, rats, orangutans, rhesus monkeys, domestic dogs and domestic cattle. Bioinformatics analysis suggested that mouse *Tmem106a* is specifically and highly expressed in peritoneal and bone marrow-derived macrophages (<http://ds.biogps.org/?gene=217203>). Further, it was shown that

the expression level of TMEM106A was significantly up-regulated in macrophages after bacterial infection (<https://www.ncbi.nlm.nih.gov/geo/profiles>). Previous research showed that mouse TMEM106A was highly expressed on the surface of peritoneal macrophages (PMs) and RAW264.7 cells [23]. Moreover, treatment with anti-mouse TMEM106A polyclonal antibodies has been shown to activate PMs, indicating that TMEM106A may play a regulatory role in immune and inflammatory responses.

In the present study, we generated *Tmem106a* knock-out (KO) mice to further investigate the immunological functions of TMEM106A. Our results demonstrated that *Tmem106a*^{-/-} mice exhibited increased sensitivity to LPS and cecal ligation puncture (CLP) treatment, accompanied by macrophage activation via the MAPK and NF- κ B signaling pathways; however, this effect was abrogated by macrophage depletion in *Tmem106a*^{-/-} mice. Additionally, clinical analysis revealed that the levels of TMEM106A in peripheral monocytes were higher in patients with sepsis than those in healthy donors. These results indicate that TMEM106A play a negative regulatory role in macrophage-mediated inflammatory response.

Materials and methods

Antibodies and reagents

Antibodies and reagents in this study are listed in the Supporting information, Tables S1 and S2.

Tmem106a gene KO mice

Tmem106a KO mice were produced using CRISPR/Cas9 genome editing with guide RNA (5'- GCTCACCTCTCGG AAGGATG-3') targeting close to the start codon in the exon 3 of mouse *Tmem106a*. C57BL/6 J \times FVB/N mouse embryos were injected with gRNAs and Cas9 mRNA at the Cornell Transgenic Core Facility. Editing was confirmed by sequencing polymerase chain reaction (PCR) products from genomic DNA. Offspring from the founder containing 148 base pairs (bp) deletion were back-crossed to a C57/BL6 background for 10 generations and used for the study. Δ 148 bp KO mice genotyping was performed by PCR using oligonucleotides 5'- TTCACTTGAGAAA TCCCTTAAA-3' and 5'- GCCAGCCTGAGACTGC ATAC-3' [wild-type (WT) allele (577 bp), mutant allele (429 bp)].

The mutant mice appeared phenotypically normal, and no obvious developmental and reproductive defects were observed. All mice were housed in a specific pathogen-free (SPF) facility at a constant room temperature with free access to water and standard mouse chow. All animal experimental procedures and techniques were approved by the Animal Ethics Committee of Peking University Health Sciences Center (LA2018266) and the Institutional

Animal Care and Use Committee at Cornell University (animal protocol 2017-0056).

Animal model

Mice (aged 8–12 weeks) were intraperitoneally injected with LPS (15 mg/kg) to induce sepsis. Control mice received the same volume of PBS.

For cecal ligation and puncture model, female mice (aged 8 weeks) were intraperitoneally anesthetized with a combination of ketamine (125 mg/kg) and xylazine (7.5 mg/kg). The cecum was exposed under sterile surgical conditions and ligated at the distal 50% position. Then, the ligated cecum was punctured by a 21G needle and a small amount of feces was gently extruded from the holes. The cecum was replaced into the peritoneal cavity and the abdomen was closed. The mice were housed in microisolators after surgery.

For macrophage depletion, mice (aged 8 weeks) were intravenously injected with clodronate liposomes (200 µl/mouse) 48 h before LPS administration to clear macrophages. The efficiency of clearance was proved by flow cytometric analysis.

Cell isolation and flow cytometry

Mice were euthanized by CO₂ asphyxiation, and T cells, B cells, monocytes, macrophages and granulocytes were separated from blood, spleen, bone marrow, lymph node and peritoneal lavage. Different cells were stained with fluorescein-labeled antibodies and analyzed by flow cytometry (FACS Aria; BD Biosciences, San Jose, CA, USA).

Human peripheral blood mononuclear cells (PBMCs) from blood were separated by Ficoll, stained with fluorescein isothiocyanate (FITC)-conjugated anti-human TMEM106A and phycoerythrin (PE)-labeled anti-human CD14 antibodies, analyzed by flow cytometry (FACS Verse; BD Biosciences). Written informed consent was received from participants prior to blood sampling and all procedures were in accordance with the Ethics Committee of Peking University Third Hospital (IRb0006761-2012015).

Bone marrow transplantations

Male and female WT mice (aged 6 weeks, $n = 10$) were fed with acidified water (pH 2.5–3) with neomycin (100 mg/l) and polymyxin B sulfate (60 000 U/l) 7 days before bone marrow transfer. Mice were fed in microbe-free irradiation boxes and subjected to a lethal dose of γ -irradiation (10 Gy). *Tmem106a*^{+/+} and *Tmem106a*^{-/-} mice were euthanized by CO₂ asphyxiation, and total bone marrow cells inside the marrow cavity were isolated by PBS flushing. Red blood cells were lysed and the remaining cells were washed twice with PBS and resuspended in

PBS containing 2% fetal calf serum (FCS) (1×10^7 cells/ml); 100 µl donor bone marrow cells were injected intravenously into the irradiated WT mice. Mice were still fed with acidified water and were housed for 8 weeks for further reconstitution and analysis.

Culture of mouse bone marrow-derived macrophages (mBMDMs)

Mouse bone marrow cells were separated and cultured in Dulbecco's modified Eagle's medium (DMEM), supplemented with macrophage colony-stimulating factor (M-CSF) and 10% Ausbian FCS for 7 days. mBMDMs were harvested with ice-cold TEN buffer [40 mM Tris, 4 mM ethylenediamine tetraacetic acid (EDTA), 0.15 M NaCl, pH 8.0] and resuspended at 5×10^5 /ml in DMEM with 10% FCS and seeded for at least 6 h prior to stimulation.

Separation of mouse peritoneal macrophages

Mice were intraperitoneally injected with 1 ml 3% (w/v) thioglycollate medium for 3 days before they were euthanized. Peritoneal macrophages were collected and resuspended at 5×10^5 /ml in DMEM with 10% FCS and seeded for at least 6 h prior to stimulation.

Construction of stable *Tmem106a* knockdown RAW264.7 cell line

The sequence of shRNA specifically targeting *Tmem106a* mRNA was 5'-GCTCAACACGACGAATGTCCT-3', which was constructed into the transfer plasmid pLVX-shRNA1. HEK 293T cells were transfected in 10 µg transfer plasmid, 6 µg packaging plasmid and 4 µg envelope plasmid; the recombinant lentiviruses were harvested and filtered 72 h post-transfection. Lentivirus-infected RAW264.7 cells were selected under pressure of 5 µg/ml puromycin.

Cytokine detection

The levels of IL-6, TNF- α and IFN- β in the serum and cell culture supernatant were measured by LEGENDplex™ mouse proinflammatory chemokine panel (740451; BioLegend, San Diego, CA, USA), according to the manufacturer's instructions.

Reverse transcription (RT)-PCR and quantitative real-time (qRT)-PCR assays

Total RNA samples were extracted from cells with the TRIzol reagent. RT-PCR was performed using the ThermoScript RT-PCR system; qRT-PCR was performed using SYBR Premix Ex Taq. The primers against the indicated genes used in this study are listed in the Supporting information, Table S3. All mouse genes expression was normalized to β -actin/*ACTB* and human genes was normalized to *GAPDH*.

Western blot analysis

All protein samples from cells were extracted by radioimmune precipitation assay (RIPA) cell lysis buffer with proteinase and phosphatase inhibitors and quantified by BCA protein assay kit. Equal-quality samples were separated by sodium dodecyl sulfate-polyacrylamide gel electrophoresis (SDS-PAGE) and transferred from gels to 0.22 μm nitrocellulose membranes. The membranes were blocked in 5% (w/v) skimmed milk in Tris-buffered saline (TBS) for 1 h and incubated with the primary antibodies at 4°C overnight. Membranes were washed and incubated with horseradish peroxidase (HRP)-conjugated primary antibodies at room temperature for 40 min. The membranes were incubated with freshly made electrochemiluminescence reagent and filmed by Amersham imager 680 (GE Healthcare, Chicago, IL, USA).

Statistical analysis

A Gehan–Breslow–Wilcoxon test was used to compare the Kaplan–Meier survival curves between the different groups of mice generated in GraphPad Prism version 6. Unpaired Student's *t*-tests (two-tailed) were performed using Prism software. A *P*-value < 0.05 was considered significant; **P* < 0.05, ***P* < 0.01 and ****P* < 0.001.

Results

Expression profile of TMEM106A in mouse and human monocytes/macrophages

We first examined the expression of TMEM106A in mouse immune cells. As shown in Fig. 1a, *Tmem106a* was highly expressed in myeloid cells, especially macrophages, as indicated by qRT-PCR. Additionally, in phorbol myristate acetate (PMA)-stimulated THP-1 macrophages, high mRNA levels of *TMEM106A* were observed (Fig. 1b). Moreover, the levels of *Tmem106a* mRNA were significantly increased in LPS-stimulated mouse bone marrow-derived macrophages (mBMDMs), as indicated by qRT-PCR (Fig. 1c). Treatment with LPS (100 ng/ml) further enhanced the protein expression of TMEM106A in PMA-stimulated THP-1 cells, as evidenced by flow cytometry (FCM) analysis (Fig. 1d,e).

We next detected the expression of TMEM106A in patients with sepsis. PBMCs were isolated from healthy donors and patients with sepsis, followed by staining with anti-CD14-PE and anti-TMEM106A-FITC antibodies. FCM analysis demonstrated that TMEM106A was mainly expressed on CD14⁺ monocytes in human blood (Fig. 1f,g), and the proportion of CD14⁺TMEM106A⁺ cells was significantly increased in patients with sepsis compared to that in normal donors. Furthermore, the mean fluorescence intensity (MFI) and the levels of *TMEM106A*

mRNA were also increased in patients with sepsis (Fig. 1h,i), indicating that TMEM106A is up-regulated in the peripheral monocytes of sepsis patients. Taken together, our data suggest that increased TMEM106A may play an important regulatory role in the inflammatory response.

Tmem106a ablation exacerbates LPS- and CLP-stimulated inflammation

To further investigate the functions of TMEM106A in inflammatory response, we generated *Tmem106a* KO (*Tmem106a*^{-/-}) mice by CRISPR-Cas9 technology (Supporting information, Fig. S1a,b). The resulting *Tmem106a*^{-/-} mice did not exhibit spontaneous phenotypes compared with age-matched *Tmem106a*^{+/+} littermate controls. FCM data indicated that there was no significant difference in the proportion and number of T cells, B cells, macrophages or neutrophils in different tissues and blood between *Tmem106a*^{+/+} and *Tmem106a*^{-/-} mice (Supporting information, Fig. S2), suggesting that *Tmem106a* deletion does not influence the development of immunocytes.

Next, we studied whether *Tmem106a* deficiency affected with LPS-induced inflammation. *Tmem106a*^{+/+} and *Tmem106a*^{-/-} mice were inoculated with a lethal dose of LPS (15 mg/kg). Survival analysis showed that, at 50 h post-inoculation, almost all *Tmem106a*^{-/-} mice died, while 80% of *Tmem106a*^{+/+} mice were alive. Overall, approximately 60% of *Tmem106a*^{+/+} mice survived after LPS challenge (Fig. 2a). Furthermore, we analyzed the serum levels of inflammatory factors after LPS (5 mg/kg) treatment for 2 h. As shown in Fig. 2b, the levels of TNF, IL-6 and IFN- β protein were significantly increased in *Tmem106a*^{-/-} mice compared with those in *Tmem106a*^{+/+} mice. The results of hematoxylin and eosin (H&E) staining indicated that the lung tissues of *Tmem106a*^{-/-} mice displayed high inflammatory cell infiltration, hemorrhage and interstitial pneumonitis after LPS (10 mg/kg) challenge for 18 h (Fig. 2c). Immunohistochemical results further demonstrated a significant increase in the number of Ly6G⁺ cells in the *Tmem106a*^{-/-} lung tissues (Fig. S3). These data indicated that *Tmem106a* may inhibit LPS-induced inflammatory responses and protect the host against inflammation.

Next, we performed cecal ligation and puncture (CLP) to further explore the function of TMEM106A in polymicrobial infections. At 40 h after CLP approximately 50% of all *Tmem106a*^{-/-} mice died, while all *Tmem106a*^{+/+} mice were alive. After 7 days of treatment, 50% of *Tmem106a*^{+/+} mice continued to survive, whereas only 20% of *Tmem106a*^{-/-} mice were alive (Fig. 2d). Corresponding to this phenotype, at 12 h after CLP, *Tmem106a*^{-/-} mice displayed higher serum levels of TNF and IL-6 protein (Fig. 2e) and showed more severe lung injury (Fig. 2f) than *Tmem106a*^{+/+} mice. Collectively, knock-out of *Tmem106a* exacerbates inflammatory tissue damage,

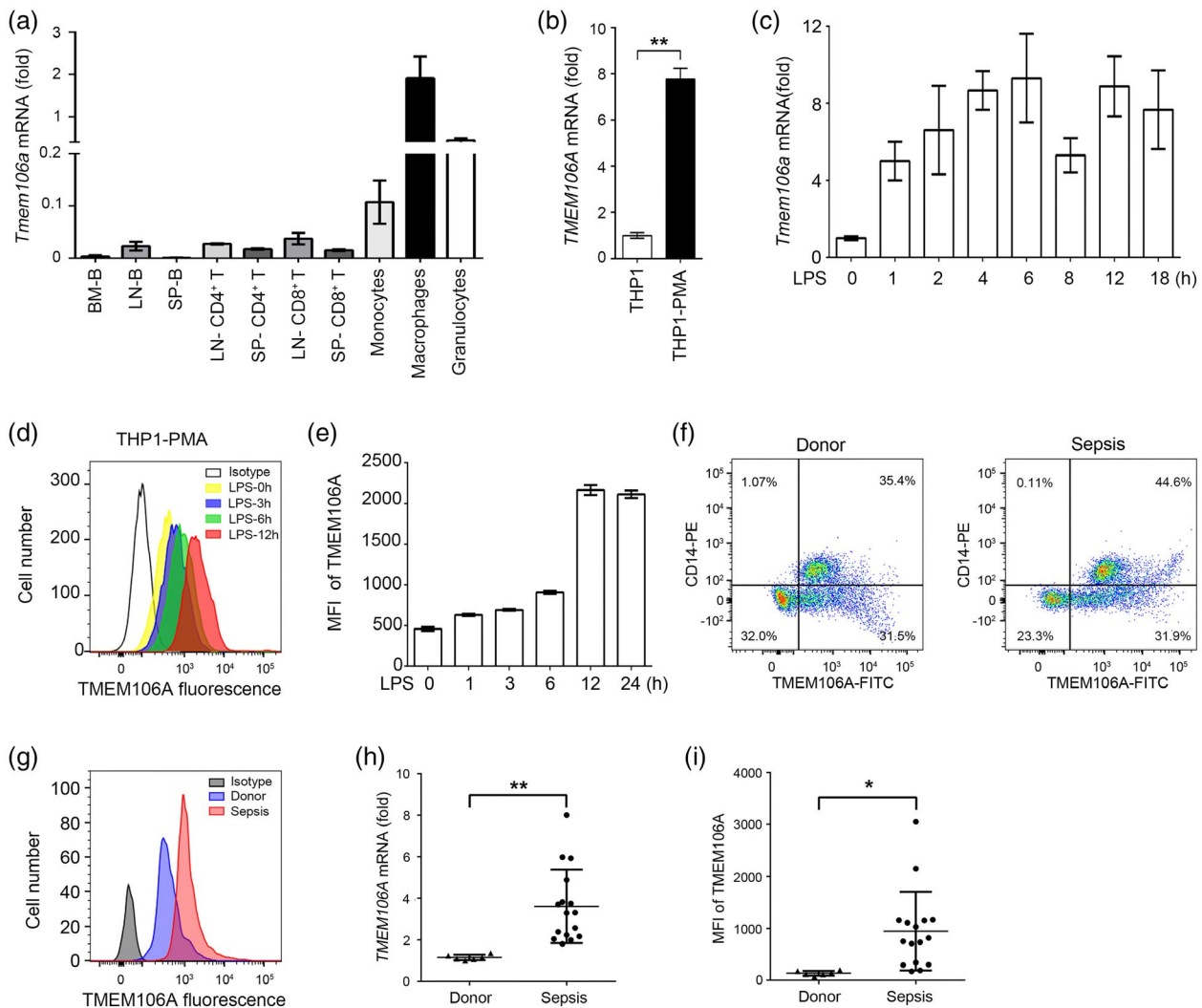


Fig. 1. Transmembrane protein 106A (TMEM106A) is highly expressed in mouse/human monocytes/macrophages. (a) Quantitative reverse transcription–polymerase chain reaction (qRT–PCR) analysis of *Tmem106a* mRNA in sorted bone marrow B (BM-B) cells, lymph node B (LN-B) cells, spleen B (SP-B) cells, lymph node CD4⁺ T (LN-CD4⁺ T) cells, spleen CD4⁺ T (SP-CD4⁺ T) cells, lymph node CD8⁺ T (LN-CD8⁺ T) cells, spleen CD8⁺ T (SP-CD8⁺ T) cells, monocytes, peritoneal macrophages and granulocytes of wild-type mice. (b) Human acute monocytic leukemia cell line (THP1) cells were treated with or without phorbol myristate acetate (PMA) (50 ng/ml) for 48 h and the levels of *TMEM106A* mRNA were analyzed by qRT–PCR. (c) Mouse bone marrow-derived macrophages (mBMDMs) were stimulated with lipopolysaccharide (LPS) (100 ng/ml) at the indicated time, the levels of *Tmem106a* mRNA were detected by qRT–PCR. (d,e) PMA-induced THP1 cells were treated with LPS (100 ng/ml) at the indicated time, stained with fluorescein isothiocyanate (FITC)-anti-TMEM106A and detected by flow cytometry (FCM) and statistically analyzed (e). (f) Peripheral blood mononuclear cells were separated from healthy donor and sepsis patient, then stained with anti-CD14-phycoerythrin (PE) and anti-TMEM106A-FITC and analyzed by flow cytometry. (g) Histogram of TMEM106A-FITC gated from CD14⁺ cells. (h) Mean fluorescence intensity (MFI) of TMEM106A-FITC gated from CD14⁺ cells. (i) The levels of *TMEM106A* mRNA in peripheral blood mononuclear cells (PBMCs) were assessed by qRT–PCR. (a–e) Dates are representative of at least three independent experiments. Mean ± standard deviation (s.d.) of six healthy donors and 16 sepsis patients are shown in (h) and (i). **P* < 0.05, ***P* < 0.01.

suggesting that TMEM106A may negatively regulate inflammatory response.

Macrophages are required for the enhanced inflammation in LPS-treated *Tmem106a* KO mice

Given that *Tmem106a* expression is silenced in all cells of *Tmem106a*^{-/-} mice, we wanted to investigate whether

macrophages are involved in *Tmem106a*-mediated effects. For this purpose, we transplanted the *Tmem106a*^{+/+} or *Tmem106a*^{-/-} bone marrow (BM) into lethally irradiated WT mice and then assessed their response to LPS. When challenged with LPS, chimeric mice reconstituted with *Tmem106a*^{-/-} BM (*Tmem106a*^{-/-} → *Tmem106a*^{+/+}) produced higher levels of TNE, IL-6 and IFN-β than those

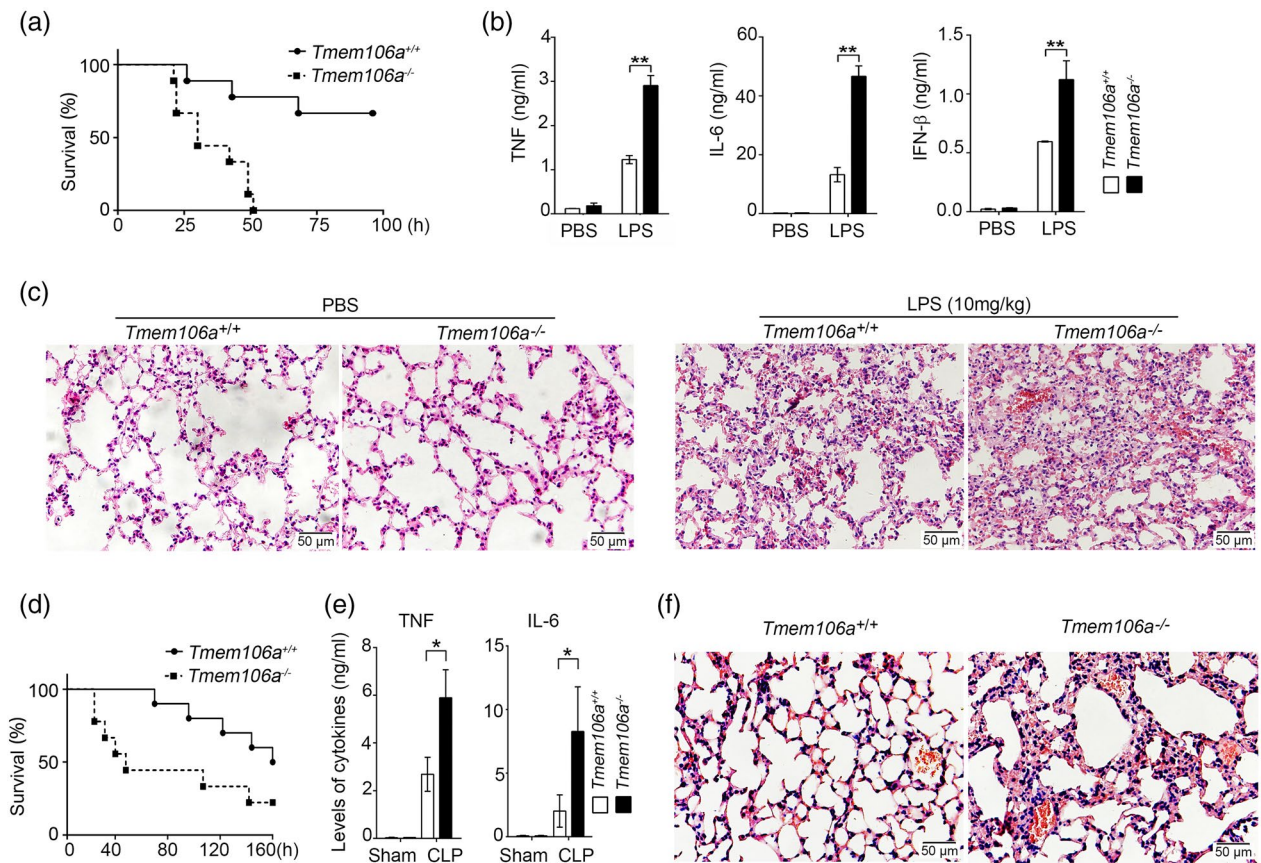


Fig. 2. *Tmem106a* knock-out (KO) mice are more sensitive to lipopolysaccharide (LPS)-induced septic shock. (a) Mice ($n = 9$) were intraperitoneally injected with LPS (15 mg/kg) or phosphate-buffered saline (PBS), observed by every 2 h, and the survival curve is outlined. (b) *Tmem106a*^{+/+} and *Tmem106a*^{-/-} mice ($n = 5$) were intraperitoneally injected with LPS (5 mg/kg), the levels of TNF, IL-6 and IFN- β in serum were detected by LEGENDplex[™] mouse proinflammatory chemokine panel after 2 h injection. (c) *Tmem106a*^{+/+} and *Tmem106a*^{-/-} mice were intraperitoneally injected with LPS (10 mg/kg), representative lung images of hematoxylin and eosin (H&E) staining from different groups were analyzed after 18 h injection. (d) Survival curve of *Tmem106a*^{+/+} and *Tmem106a*^{-/-} mice ($n = 9$) subjected to cecal ligation and puncture (CLP). (e) Serum levels of TNF and IL-6 in mice 12 h after sham or CLP surgery. (f) H&E staining of lung in *Tmem106a*^{+/+} and *Tmem106a*^{-/-} mice 24 h after CLP surgery. Above data are representative of at least three independent experiments. * $P < 0.05$, ** $P < 0.01$.

reconstituted with *Tmem106a*^{+/+} BM (Fig. 3a). Next, in order to determine whether TMEM106A⁺ macrophages are the primary cause of LPS-stimulated responses, *Tmem106a*^{+/+} or *Tmem106a*^{-/-} mice were intravenously injected with clodronate liposomes for 48 h, and the proportion of CD11b⁺F4/80⁺ macrophages in the peritoneal cavity was analyzed by FCM. As showed in Fig. 3b,c, liposome administration significantly decreased the proportion and number of PMs, indicating the effective clearance of mouse macrophages. Following this, mice were subjected to LPS stimulation. As illustrated in Fig. 3d, the serum levels of TNF, IL-6 and IFN- β were significantly reduced in both liposome-treated *Tmem106a*^{+/+} and *Tmem106a*^{-/-} mice after LPS challenge. The above data demonstrated that depletion of macrophages decreased LPS-stimulated inflammation in *Tmem106a*^{-/-} mice,

suggesting that macrophages are required for the enhanced inflammation in LPS-treated *Tmem106a* KO mice.

Tmem106a deletion promotes macrophage activation and polarization towards M1 phenotype

Considering that macrophages are the main mediators of TLR-induced inflammatory responses *in vivo*, we assessed the effect of LPS stimulation on *Tmem106a*^{-/-} macrophages. Consistent with the *in-vivo* data presented above, *Tmem106a*^{-/-} PMs produced higher levels of TNF and IL-6 protein than *Tmem106a*^{+/+} PMs in response to LPS (100 ng/ml) treatment (Fig. 4a). Their transcript levels were also markedly increased at different time-points after LPS challenge (Supporting information, Fig. S4a). Similar results were obtained in mBMDMs from *Tmem106a*^{-/-} mice (Fig. 4b and Supporting information, Fig. S4b). *Tmem106a*-silenced RAW264.7 cells established by

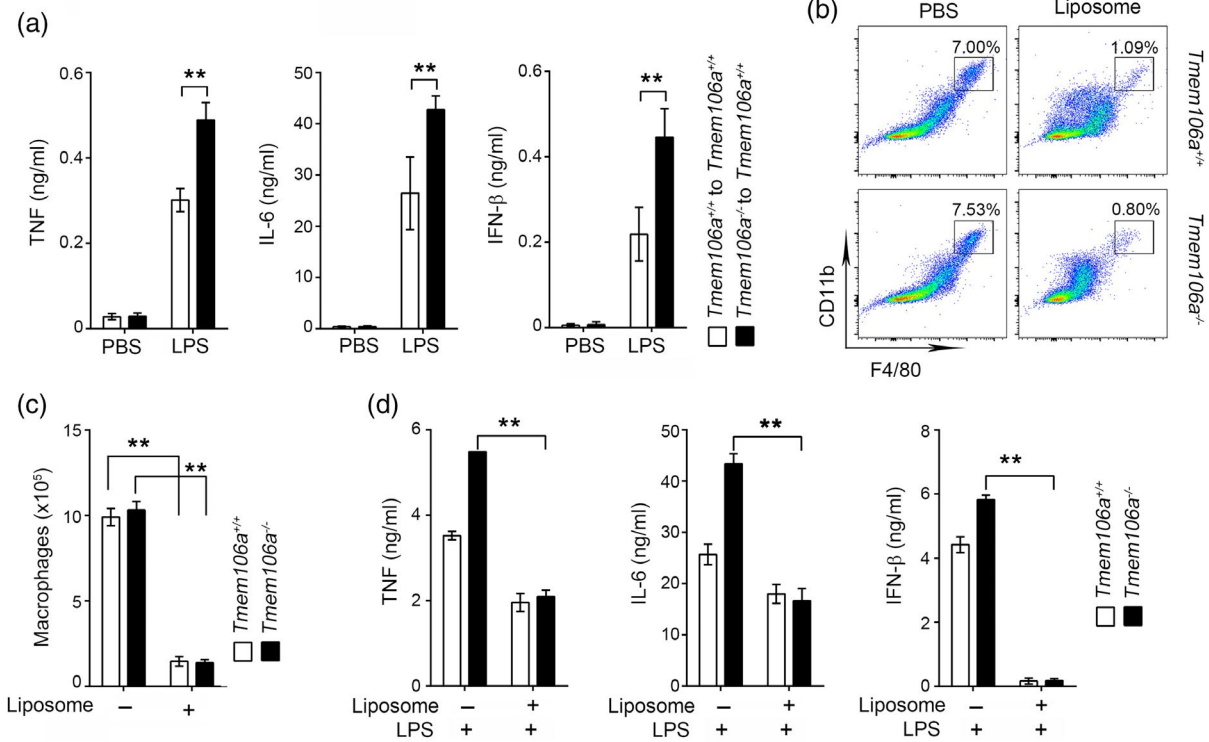


Fig. 3. Macrophages are required for the enhanced inflammation in lipopolysaccharide (LPS)-treated *Tmem106a* knock-out (KO) mice. (a) *Tmem106a*^{+/+} or *Tmem106a*^{-/-} bone marrow (BM) were transplanted into lethally irradiated wild-type mice (10 Gy), respectively. Eight weeks later, reconstituted chimeric mice ($n = 5$) were challenged with phosphate-buffered saline (PBS) or LPS (5 mg/kg) for 2 h. The levels of tumor necrosis factor (TNF), interleukin (IL)-6 and interferon (IFN)- β in serum were detected. (b,c) *Tmem106a*^{+/+} and *Tmem106a*^{-/-} mice were intravenously injected with 200 μ l PBS or clodronate liposomes for 48 h. The proportions and number of CD11b⁺F4/80⁺ cells in the peritoneal cavity were detected by flow cytometry and statistically analyzed. (d) *Tmem106a*^{+/+} and *Tmem106a*^{-/-} mice ($n = 6$) were injected with or without clodronate liposome for 48 h, followed by LPS (5 mg/kg) for 2 h and the levels of TNF, IL-6 and IFN- β in serum were measured. ** $P < 0.01$.

infection with *pLVX-shTmem106a* exhibited significantly reduced *Tmem106a* expression compared to cells infected with empty *pLVX-shcontrol* (Supporting information, Fig. S4c). After treatment with LPS, the *pLVX-shTmem106a*-infected cells displayed higher protein and mRNA levels of TNF and IL-6 (Fig. 4c and Supporting information, Fig. S4d), similar to those of *Tmem106a*^{-/-} macrophages. These results indicate that the inactivation of *Tmem106a* gene sensitizes cells to LPS response, and the cytokine secretion profiles of *Tmem106a*^{-/-} macrophages are consistent with the M1 phenotype.

Typically, M1 macrophages are characterized by high expression of proinflammatory cytokines and strong phagocytosis activity. Experimental data suggested that *Tmem106a*-silenced RAW264.7 cells displayed no significant phagocytosis activities (Supporting information, Fig. S5a–c). Similar results were obtained for *Tmem106a*^{-/-} mBMDMs (Supporting information, Fig. S5d–f). To analyze the effects of TMEM106A on macrophage activation, mBMDMs from *Tmem106a*^{+/+} and *Tmem106a*^{-/-} mice were

incubated with or without LPS (100 ng/ml) for 24 h before staining with anti-mouse CD80, CD86 or MHC-II antibodies, followed by FCM analysis (Supporting information, Fig. S6a). Results showed that, compared with LPS-treated *Tmem106a*^{+/+} mBMDMs, LPS-treated *Tmem106a*^{-/-} mBMDMs displayed up-regulation of CD80, CD86 and MHC-II protein (Supporting information, Fig. S6a and Fig. 4d). The same experiment was performed in *Tmem106a*-silenced RAW264.7 cells, and the results were similar to those for mBMDMs (Supporting information, Fig. S6b,c), indicating that the macrophages were over-activated in *Tmem106a* KO conditions.

Next, we analyzed whether TMEM106A affects the expression of CD206, a marker of M2 macrophages. As shown in Supporting information, Fig. S7a,b, after incubation with IL-4 for 24 h, the expression of CD206 was analogous between *Tmem106a*^{+/+} and *Tmem106a*^{-/-} mBMDMs. The same results were obtained for IL-4-treated RAW264.7 cells (Supporting information, Fig. S7c,d), indicating that *Tmem106a* deletion does not influence M2 macrophages.

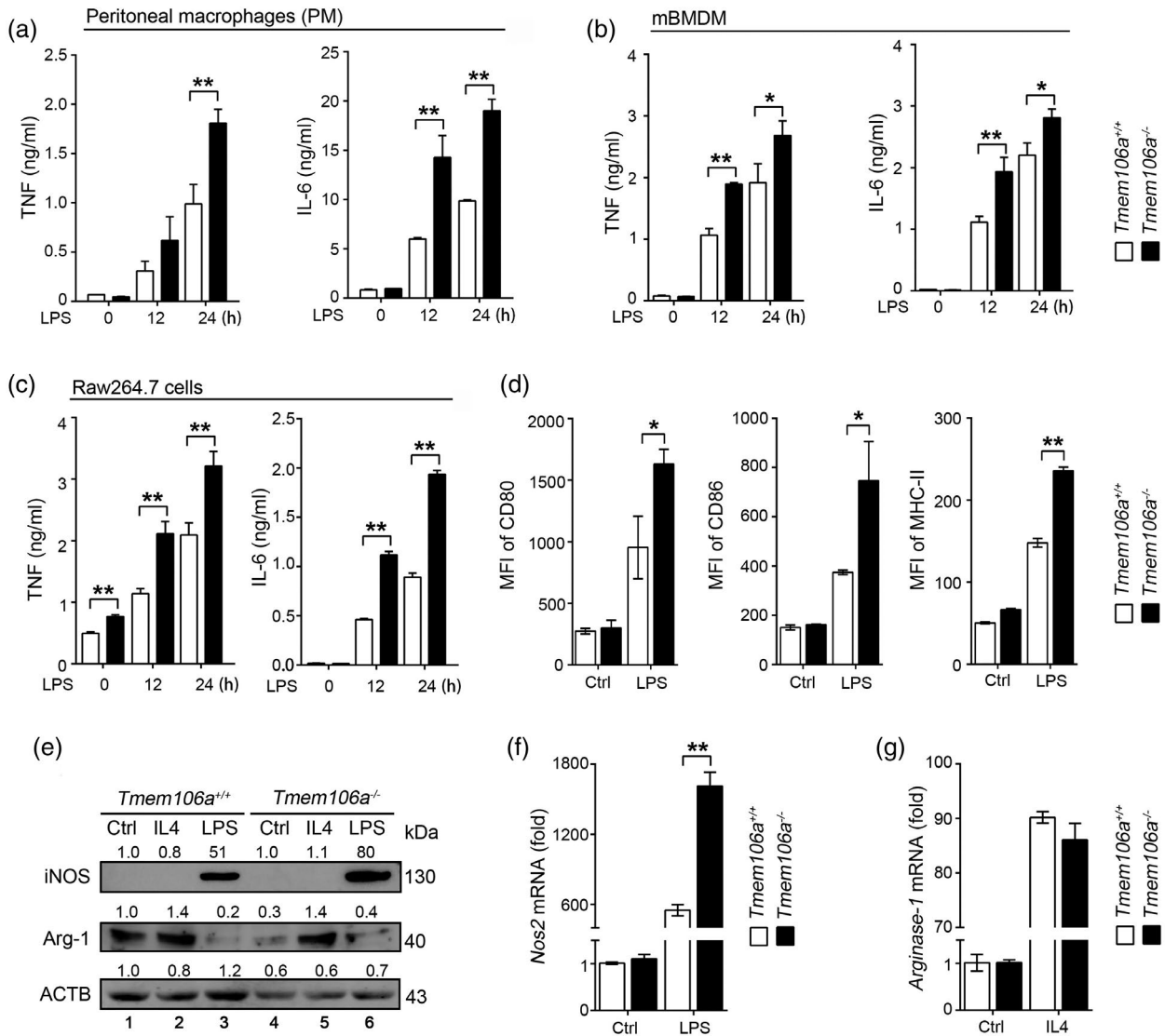


Fig. 4. *Tmem106a* deletion promotes macrophage activation and polarization towards the M1 phenotype. (a,b) *Tmem106a*^{+/+} and *Tmem106a*^{-/-} peritoneal macrophages (PMs) (a) or mouse bone marrow-derived macrophages (mBMDMs) (b) were stimulated with or without lipopolysaccharide (LPS) (100 ng/ml) at the indicated time and the levels of tumor necrosis factor (TNF) and interleukin (IL)-6 in the supernatant were measured, respectively. (c) Levels of TNF and IL-6 in the supernatant in control and *Tmem106a* knockdown RAW264.7 cells stimulated with or without LPS (100 ng/ml) at the indicated time. (d) *Tmem106a*^{+/+} and *Tmem106a*^{-/-} mBMDMs were stimulated with or without LPS (100 ng/ml) at 24 h. The levels of CD80, CD86 and major histocompatibility complex (MHC)-II were detected by flow cytometry and the mean fluorescence intensity (MFI) was statistically analyzed. (e) *Tmem106a*^{+/+} and *Tmem106a*^{-/-} PMs were treated with or without 100 ng/ml of LPS (or 10 ng/ml of IL-4) for 24 h, the levels of inducible nitric oxide synthase (iNOS) and arginase 1 (Arg-1) were measured by Western blot. A representative blot and the relative gray values are shown. (f,g) *Tmem106a*^{+/+} and *Tmem106a*^{-/-} PMs were treated as same as (e), the levels of *Nos2* and *Arginase-1* mRNA were measured by quantitative reverse transcription–polymerase chain reaction (qRT-PCR). **P* < 0.05, ***P* < 0.01.

To further characterize the changes in macrophage polarization, we assessed the expression of the M1 marker [inducible nitric oxide synthase (iNOS)] and the M2 marker [arginase-1 (Arg-1)]. Both *Tmem106a*^{+/+} and *Tmem106a*^{-/-} PMs were cultured with or without LPS (or IL-4) for 24 h. Western blot analysis indicated that, compared with LPS-treated *Tmem106a*^{+/+} PMs,

LPS-treated *Tmem106a*^{-/-} PMs showed enhanced expression of iNOS (Fig. 4e). Further, qRT-PCR data demonstrated that *Tmem106a*^{-/-} PMs displayed higher mRNA levels of NOS2 than *Tmem106a*^{+/+} PMs (Fig. 4f). In response to IL-4 treatment, no alteration in Arg-1 expression was observed between the *Tmem106a*^{+/+} and *Tmem106a*^{-/-} groups (Fig. 4e,g). Taken together, these

results suggest that *Tmem106a* deficiency promotes LPS-mediated polarization towards M1 macrophages.

***Tmem106a* deletion promotes activation of the MAPK and NF- κ B signaling pathways in macrophages during LPS stimulation**

LPS, a well-known TLR-4 ligand, can activate downstream TLR-4 signaling pathways, such as the MAPK and NF- κ B pathways, to induce the transcription of various inflammatory cytokines. To the possible mechanism underlying TMEM106A-regulated macrophage activation, PMs from *Tmem106a*^{+/+} and *Tmem106a*^{-/-} mice were stimulated with 100 ng/ml LPS for the indicated times. The levels of total and phosphorylated MAPKs and NF- κ B p65 were then assessed by immunoblotting. As shown in Fig. 5a–e, compared with LPS-treated *Tmem106a*^{+/+} PMs, LPS-treated *Tmem106a*^{-/-} PMs showed a significant increase in the levels of phosphorylated p38 MAPK, extracellular signal-regulated kinase (ERK), JUN N-terminal kinase (JNK) and NF- κ B p65, indicating an increased activation of MAPK and NF- κ B signaling in *Tmem106a*^{-/-} PMs.

As the nuclear translocation of NF- κ B p65 is a key indicator of the activation of the NF- κ B signaling pathway, we next examined the distribution of the NF- κ B p65 subunit in mouse PMs by confocal microscopy. Compared with those in *Tmem106a*^{+/+} PMs, the fluorescence intensity and nuclear distribution of NF- κ B p65 subunit were obviously increased in *Tmem106a*^{-/-} macrophages (Supporting information, Fig. S8), thus confirming NF- κ B pathway activation.

To further confirm whether MAPK and NF- κ B signals are required for *Tmem106a*-induced macrophage activation, PD98059 (an MEK1/2 inhibitor) and JSH-23 (an NF- κ B inhibitor) were employed (Supporting information, Fig. S9a,b). Both *Tmem106a*^{+/+} and *Tmem106a*^{-/-} PMs were pretreated with control or PD98059 for 2 h, followed by stimulation with LPS for the indicated times. qRT-PCR results showed that pretreatment with PD98059 significantly reduced LPS-induced *Tnf*, *Il-6* and *Ifn- β* mRNA levels in both *Tmem106a*^{+/+} and *Tmem106a*^{-/-} PMs (Fig. 5f–h). Simultaneously, under the same conditions, JSH-23 pretreatment also attenuated LPS-induced expression of the above-mentioned cytokines (Fig. 5i–k). These data indicate that *Tmem106a*^{-/-} macrophage activation, at least partially, is mediated via the MAPK and NF- κ B signaling pathways.

Discussion

In this study, we explored the role of TMEM106A in innate immune responses *in vivo* and *in vitro*. Experimental data demonstrated that the expression of TMEM106A was increased in both mouse and human macrophages with

or without LPS stimulation, as well as in patients with sepsis. Moreover, genetic deletion of *Tmem106a* enhanced macrophage activation through the MAPK and NF- κ B signaling pathways, leading to increased production of proinflammatory cytokines and iNOS, consequently exacerbating LPS- and CLP-stimulated inflammation. However, these effects were abrogated by macrophage deletion in *Tmem106a*^{-/-} mice. Thus, our results suggested that TMEM106A negatively regulated monocyte/macrophage-mediated inflammatory responses, and may serve a protective role in the context of inflammatory diseases or pathogen infections.

Macrophage polarization has been shown to be plastic and reversible. While M1 polarization occurs at the initial stages of inflammation, M2 polarization is predominant during the resolution phases of inflammation. The sequential occurrence of both polarization states is an absolute requirement for the appropriate termination of inflammation, as well as for adequate tissue repair after injury [24]. In the present study, we found that *Tmem106a* deficiency enhanced the levels of proinflammatory cytokines, such as TNF and IL-6 in LPS-stimulated macrophages, accompanied by the upregulation of CD80, CD86, MHC-II and iNOS, which are markers of M1 macrophages. This finding supported the notion that *Tmem106a* deletion induces polarization of macrophages towards the proinflammatory M1 phenotype. Efficient M1 macrophage responses are important for ensuring resistance to bacterial infection and are elicited to control pathogen growth. Conversely, excessive or unresolved M1 macrophage activation can lead to acute/chronic inflammation and tissue damage. Our study demonstrated that *Tmem106a*^{-/-} macrophages had no influence on phagocytosis compared to *Tmem106a*^{+/+} cells (Supporting information, Fig. S5), implying that TMEM106A might not regulate the phagocytic activities of macrophages. Conversely, *Tmem106a*^{-/-} mice displayed high inflammatory cell infiltration, hemorrhage and interstitial pneumonitis in the lungs after LPS challenge, eventually leading to a decline in survival. CLP experiments (Fig. 2d–f), further supporting the finding that TMEM106A inactivation exacerbates tissue damage. Our studies suggested that TMEM106A may restrict inflammatory responses after LPS stimulation or bacterial infection and protect the host against inflammation. Additionally, whether TMEM106A is associated with antigen processing, transport or presentation in macrophages needs further investigation.

TLRs can be activated by various types of stimuli, such as pathogens, different cytokines or certain cellular stresses. LPS is the main ligand for TLR-4. The LPS–TLR-4 complex binds to CD14, which can enhance TLR-4 signaling by facilitating its transport to lipid rafts in the cell membrane. Following this, MD2 is recruited to promote the translocation of TLR-4 to the cell membrane. LPS recognition

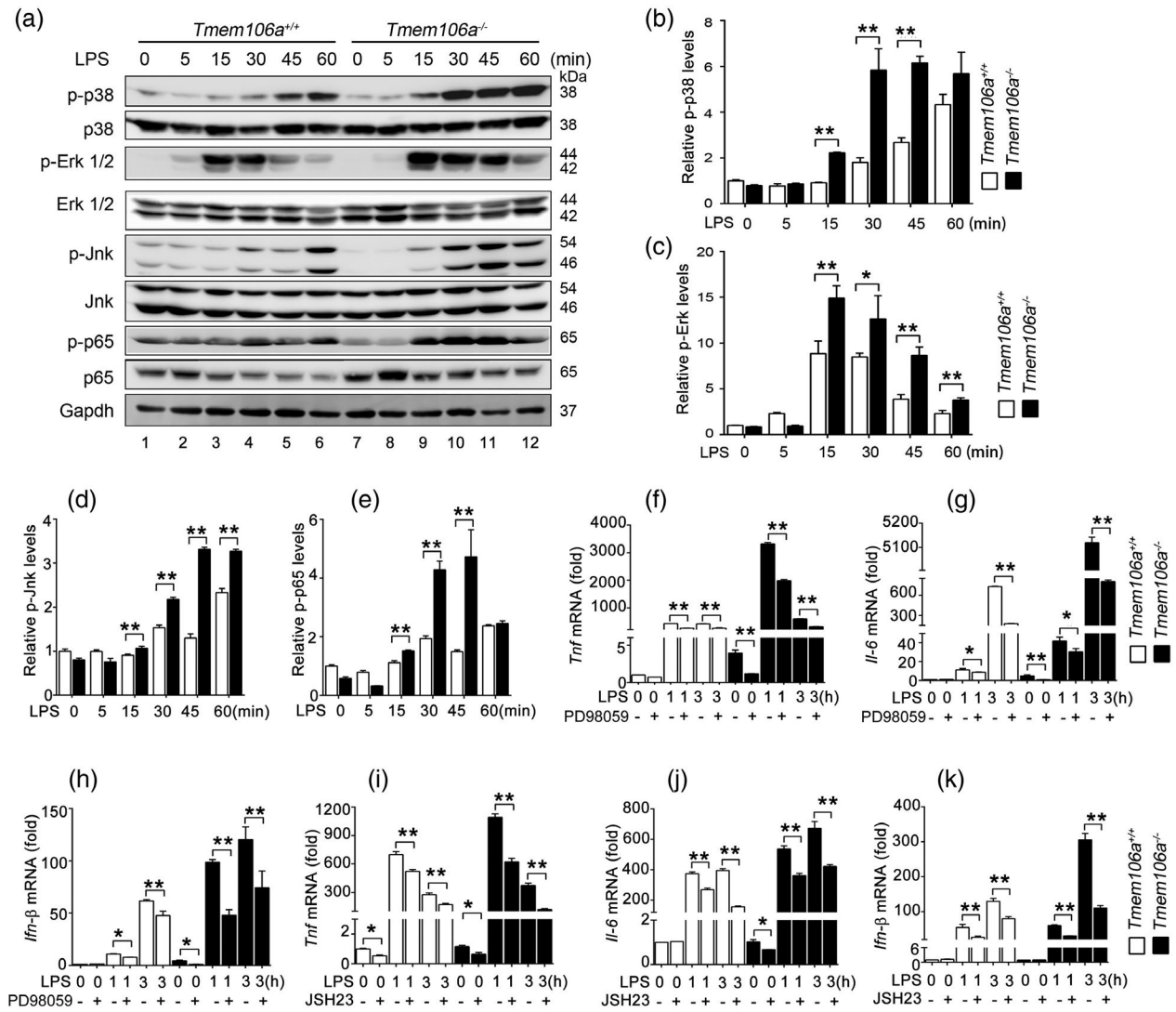


Fig. 5. *Tmem106a* deletion promotes lipopolysaccharide (LPS)-triggered mitogen-activated protein kinase (MAPK) and nuclear factor kappa B (NF-κB) signaling pathways. (a) *Tmem106a*^{+/+} and *Tmem106a*^{-/-} PMs were stimulated with LPS (100 ng/ml) at the indicated time and analyzed with Western blot at the indicated protein levels. (b–e) Quantification of indicated protein levels relative to glyceraldehyde 3-phosphate dehydrogenase (GAPDH) treated as described in (a). Average value of *Tmem106a*^{+/+} mice without LPS was normalized to 1. (f–h) *Tmem106a*^{+/+} and *Tmem106a*^{-/-} PMs were pretreated with or without 50 μM of PD98059 or 50 μM of JSH23 (i–k), respectively. Two hours later, cells were stimulated with 100 ng/ml of LPS for the indicated time, and the levels of *Tnf*, *Il6* and *Ifn-β* mRNA were detected by quantitative reverse transcription–polymerase chain reaction (qRT-PCR). **P* < 0.05, ***P* < 0.01.

by the heterotrimer CD14/TLR-4/MD2 induces activation of the MyD88-dependent and -independent pathways [25]. MyD88 associates with the IL-1 receptor associated kinase/TNFR-associated factor 6 (IRAK/TRAF6) and of transforming growth factor β activated kinase 1/TAK1 binding proteins (TAK1/TABs) complex, leading to the activation of inhibitor of nuclear factor kappa B kinase (IKK). Then, IKK phosphorylates NF-κB inhibitor alpha (IκBα), which stimulates the nuclear translocation of NF-κB which, in turn, induces the activation of proinflammatory cytokines and type I interferons [26]. TAK1 is also associated with

the MAPK pathway and stimulates the activation of p38, JNK and ERK1/2, which leads to the nuclear translocation of AP-1 and transcription of proinflammatory cytokines. Here, we demonstrated that in *Tmem106a*^{-/-} macrophages, activation of MAPK and NF-κB was increased after LPS treatment. Moreover, this effect was decreased by treatment with MEK1/2 or NF-κB inhibitor, indicating that TMEM106A-regulated macrophage activation is, at least partially, mediated via the MAPK and NF-κB signaling pathways. Considering that mouse *Tmem106a* was highly expressed on the surface of PMs and RAW264.7 cells

[23], we suggested that TMEM106A might act as an upstream of LPS-TLR4 signaling pathway. However, to elucidate the exact molecular mechanism by which TMEM106A regulates macrophage activation, further studies are needed in the future.

In summary, our findings provide insight into the regulatory activities of TMEM106A on monocyte/macrophage-mediated inflammatory responses. Our study identifies that high expression of TMEM106A may serve a protective role in the context of inflammatory diseases or pathogen infections. Further experiments are required to elucidate the physical and functional relationship between TMEM106A and macrophages under different conditions.

Acknowledgements

This work was supported by grants from the Beijing Natural Science Foundation (7192094), the National Natural Science Foundation of China (31872827, 91954116).

Disclosures

None of the authors have any conflicts of interest in relation to the content of the present work.

Data availability statement

The data that support the findings of this study are available from the corresponding author upon reasonable request.

Reference

- Gentek R, Molawi K, Sieweke MH. Tissue macrophage identity and self-renewal. *Immunol Rev* 2014; **262**:56–73.
- Bennett ML, Bennett FC. The influence of environment and origin on brain resident macrophages and implications for therapy. *Nat Neurosci* 2020; **23**:157–66.
- Krenkel O, Tacke F. Liver macrophages in tissue homeostasis and disease. *Nat Rev Immunol* 2017; **17**:306–21.
- Bronte V, Murray PJ. Understanding local macrophage phenotypes in disease: modulating macrophage function to treat cancer. *Nat Med* 2015; **21**:117–9.
- Akira S, Uematsu S, Takeuchi O. Pathogen recognition and innate immunity. *Cell* 2006; **124**:783–801.
- Triantafyllou M, Triantafyllou K. Lipopolysaccharide recognition: CD14, TLRs and the LPS-activation cluster. *Trends Immunol* 2002; **23**:301–4.
- Bode JG, Ehltling C, Haussinger D. The macrophage response towards LPS and its control through the p38(MAPK)–STAT3 axis. *Cell Signal* 2012; **24**:1185–94.
- Rosol M, Heine H, Meusch U *et al.* LPS-induced cytokine production in human monocytes and macrophages. *Crit Rev Immunol* 2011; **31**:379–446.
- Akira S, Takeda K. Toll-like receptor signalling. *Nat Rev Immunol* 2004; **4**:499–511.
- Rosadini CV, Kagan JC. Early innate immune responses to bacterial LPS. *Curr Opin Immunol* 2017; **44**:14–9.
- Shirey KA, Lai W, Scott AJ *et al.* The TLR4 antagonist Eritoran protects mice from lethal influenza infection. *Nature* 2013; **497**:498–502.
- Hammad H, Chieppa M, Perros F, Willart MA, Germain RN, Lambrecht BN. House dust mite allergen induces asthma via Toll-like receptor 4 triggering of airway structural cells. *Nat Med* 2009; **15**:410–6.
- Ferwerda B, McCall MB, Verheijen K *et al.* Functional consequences of Toll-like receptor 4 polymorphisms. *Mol Med* 2008; **14**:346–52.
- Zeng X, Liu G, Peng W *et al.* Combined deficiency of SLAMF8 and SLAMF9 prevents endotoxin-induced liver inflammation by downregulating TLR4 expression on macrophages. *Cell Mol Immunol* 2020; **17**:153–62.
- Perkins DJ, Richard K, Hansen AM *et al.* Autocrine-paracrine prostaglandin E2 signaling restricts TLR4 internalization and TRIF signaling. *Nat Immunol* 2018; **19**:1309–18.
- Chuang TH, Ulevitch RJ. Triad3A, an E3 ubiquitin-protein ligase regulating Toll-like receptors. *Nat Immunol* 2004; **5**:495–502.
- Keck S, Freudenberg M, Huber M. Activation of murine macrophages via TLR2 and TLR4 is negatively regulated by a Lyn/PI3K module and promoted by SHIP1. *J Immunol* 2010; **184**:5809–18.
- Boone DL, Turer EE, Lee EG *et al.* The ubiquitin-modifying enzyme A20 is required for termination of Toll-like receptor responses. *Nat Immunol* 2004; **5**:1052–60.
- Mansell A, Smith R, Doyle SL *et al.* Suppressor of cytokine signaling 1 negatively regulates Toll-like receptor signaling by mediating Mal degradation. *Nat Immunol* 2006; **7**:148–55.
- Xu D, Qu L, Hu J *et al.* Transmembrane protein 106A is silenced by promoter region hypermethylation and suppresses gastric cancer growth by inducing apoptosis. *J Cell Mol Med* 2014; **18**:1655–66.
- Wu C, Xu J, Wang H *et al.* TMEM106a is a novel tumor suppressor in human renal cancer. *Kidney Blood Press Res* 2017; **42**:853–64.
- Liu J, Zhu H. TMEM106A inhibits cell proliferation, migration, and induces apoptosis of lung cancer cells. *J Cell Biochem* 2018. <https://doi.org/10.1002/jcb.28057>.
- Dai H, Xu D, Su J, Jang J, Chen Y. Transmembrane protein 106a activates mouse peritoneal macrophages via the MAPK and NF- κ B signaling pathways. *Sci Rep* 2015; **5**:12461.
- Mills CD, Harris RA, Ley K. Macrophage polarization: decisions that affect health. *J Clin Cell Immunol* 2015; **6**:364.

- 25 Płóciennikowska A, Hromada-Judycka A, Borzęcka K, Kwiatkowska K. Co-operation of TLR4 and raft proteins in LPS-induced pro-inflammatory signaling. *Cell Mol Life Sci* 2015; **72**:557–81.
- 26 Taguchi T, Mukai K. Innate immunity signalling and membrane trafficking. *Curr Opin Cell Biol* 2019; **59**:1–7.

Supporting Information

Additional supporting information may be found in the online version of this article at the publisher's web site:

Fig. S1. CRISPR/Cas9 genome editing of mouse *Tmem106a*. (a) The genomic structure of wildtype and mutant *Tmem106a* gene is shown. The boxes represent exons of *Tmem106a*, and the targeting sites are shown. (b) Genomic PCR and RT-PCR were used to identify the mutations of *Tmem106a* in mice.

Fig. S2. *Tmem106a*-deficiency failed to affect the development of immunocytes. FCM analysis the proportion of CD45⁺CD4⁺ T cells(a), CD45⁺CD8⁺ T cells(b), CD45⁺CD19⁺ B cells (c), CD45⁺CD11b⁺ F4/80⁺ macrophages(d), CD45⁺CD11b⁺Ly6G⁺ neutrophils(e) in the indicated tissues between *Tmem106a*^{+/+} and *Tmem106a*^{-/-} mice (*n* = 5).

Fig. S3. The number of Ly6G⁺ cells were increased in *Tmem106a*^{-/-} lung tissues. *Tmem106a*^{+/+} and *Tmem106a*^{-/-} mice (*n* = 5) were intraperitoneally injected with LPS (10 mg/kg), Ly6G⁺ cells in lung tissues were detected by an immunohistochemical analysis.

Fig. S4. *Tmem106a*-deficiency increases the mRNA levels of pro-inflammatory cytokines in LPS-treated macrophages. *Tmem106a*^{+/+} and *Tmem106a*^{-/-} PMs (a) or mBMDMs (b) were stimulated with or without LPS (100 ng/ml) at the indicated time. The levels of both *Tnf* and *Il6* mRNA in cells were measured by qRT-PCR, respectively. (c and d) RAW264.7 cells that stably silenced *Tmem106a* with *pLVX-shTmem106a* infection or control cells were stimulated with 100 ng/ml of LPS at the indicated time. The levels of *Tmem106a* (c), *Tnf* and *Il6* mRNA were analyzed by qRT-PCR. Data are representative of at least three independent experiments. **P* < 0.05; ***P* < 0.01.

Fig. S5. *Tmem106a*-deficiency has no phagocytosis activity of macrophages. (a) RAW264.7 cells that stably silenced *Tmem106a* with *pLVX-shTmem106a* infection or control cells were cultured with RFP-*E. coli* for 3 h. The representative fluorescence images were shown. (b and c) RAW264.7 cells were treated as same as (a), cell fluorescence was detected by flow cytometry and statistically analyzed. (d) *Tmem106a*^{+/+}

and *Tmem106a*^{-/-} PMs were cultured with RFP-*E. coli* for 3 h. The representative microscope images were shown. (e and f) PMs were treated as same as (d), cell fluorescence was detected by flow cytometry and statistically analyzed. Data are representative of at least three independent experiments.

Fig. S6. *Tmem106a*-deficiency promotes the activation of M1 macrophage. (a) *Tmem106a*^{+/+} and *Tmem106a*^{-/-} mBMDMs were stimulated with or without LPS (100 ng/ml) at 24 h. The levels of CD80, CD86 and MHC-II were detected by flow cytometry. (b) RAW264.7 cells that stably silenced *Tmem106a* with *pLVX-shTmem106a* infection or control cells were treated with or without LPS (100 ng/ml) for 24 h, stained by anti-CD80 antibody and detected by flow cytometry. (c) The treatment of RAW264.7 was as same as (b), the mean fluorescence intensity (MFI) of CD80 was statistically analyzed. ***P* < 0.01.

Fig. S7. *Tmem106a*-deficiency does not influence M2 macrophages. (a and b) mBMDMs were treated with 10 ng/ml of IL4 for 24 h, stained by anti-CD206 antibody and detected by flow cytometry (a), and the MFI of CD206 was statistically analyzed (b). (c) RAW264.7 cells that stably silenced *Tmem106a* with *pLVX-shTmem106a* infection or control cells were treated with or without 10 ng/ml of IL4 for 24 h, the expression of CD206 was detected by flow cytometry. (d) The MFI of CD206 was statistically analyzed. Data are representative of at least three independent experiments.

Fig. S8. *Tmem106a* knockout promotes nuclear distribution of NF-κB p65 in macrophages triggered by LPS. *Tmem106a*^{+/+} and *Tmem106a*^{-/-} peritoneal macrophages were stimulated with 100 ng/ml of LPS for 45 minutes, stained by anti- NF-κB p65 antibody and observed by fluorescence microscopy. Cell nuclei were stained with Hoechst 33342.

Fig. S9. Effects of inhibitors on ERK and NF-κB signaling pathways in mouse macrophages. (a) *Tmem106a*^{+/+} and *Tmem106a*^{-/-} PMs were pretreated with or without 50 μM of PD98059 for 2 h, then, stimulated with 100 ng/ml of LPS for indicated time. The levels of indicated protein were analyzed by western blotting. (b) *Tmem106a*^{+/+} and *Tmem106a*^{-/-} PMs were pretreated with or without 50 μM of JSH23 for 2 h, then, stimulated with 100 ng/ml of LPS for indicated time. The levels of indicated protein were analyzed by western blotting.

Table S1. Antibodies were listed in this study

Table S2. Reagents were listed in this study

Table S3. Primers used for genome PCR and RT-qPCR